LAIDLAW RESEARCH PROJECT

The Ocean Dynamics of Icy Moons

Thenu Kaluarachchige — 31.08.2024

Supervised by

Dr Daphné Lemasquerier

kktsk1@st-andrews.ac.uk

The full report can be found at tinyurl.com/ThenuK

1 Introduction

The icy moons of Jupiter and Saturn likely harbour vast oceans of salty water beneath an icy crust, as suggested by their highly variable magnetic fields [6]. The Galilean icy moon Europa is one such example that has garnered much interest due its potential to host life. This project explores the interesting ice-ocean dynamics that could be present on an icy moon due to a non uniform temperature distribution at the ocean floor. Pinning down the ocean dynamics and salt transport of these moons may prove instrumental in ascertaining their habitability [11].

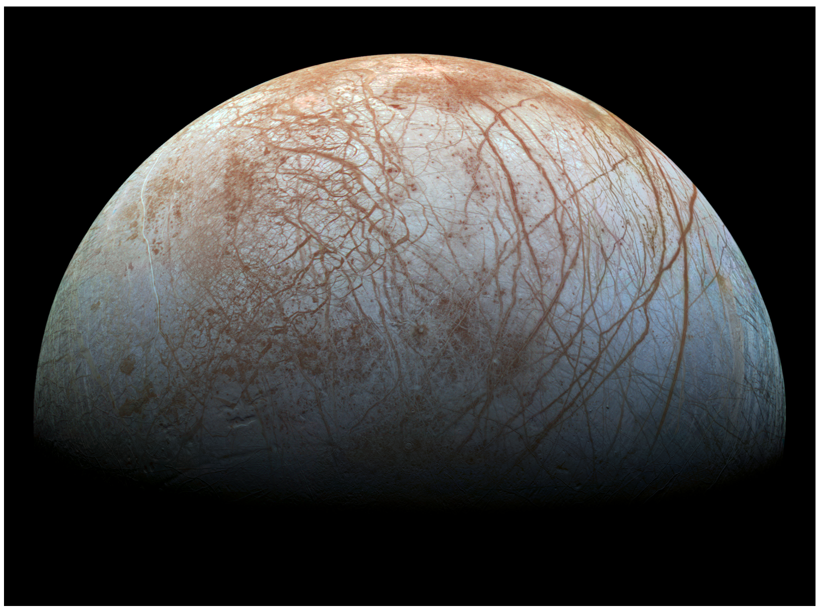

Fig 1: Europa with visible surface linea. Image credited to NASA/JPL-Caltech [9].

Evidence of Europa's oceanic system also comes from the distribution of its surface linea (see **Fig 1**). The linea are cracks on the exterior ice surface due to tidal stresses that would typically appear on the equator. The fact that we find them scattered across the surface indicates that the ice layer is likely detached from the rest of the planet and floats on top the ocean [5]. The ice layer rotates gradually, spreading the linea across the surface.

1.1 Tidal Heating

The temperature distribution of Europa's ocean floor is maintained by its elliptical orbit around Jupiter. Drawing a radial line from Jupiter through a cross section of Europa, we label the Jovian and anti-Jovian points as the closest and furthest points from Jupiter within the cross section, respectively. Gravity is a function of radial distance and the moon clearly experiences different forces at the Jovian and anti-Jovian points. As Europa moves around its elliptical orbit, the two points experience another variation in gravitational force. This effect deforms the moon along the radial line and induces heating in Europa's solid layers, including its mantle [8].

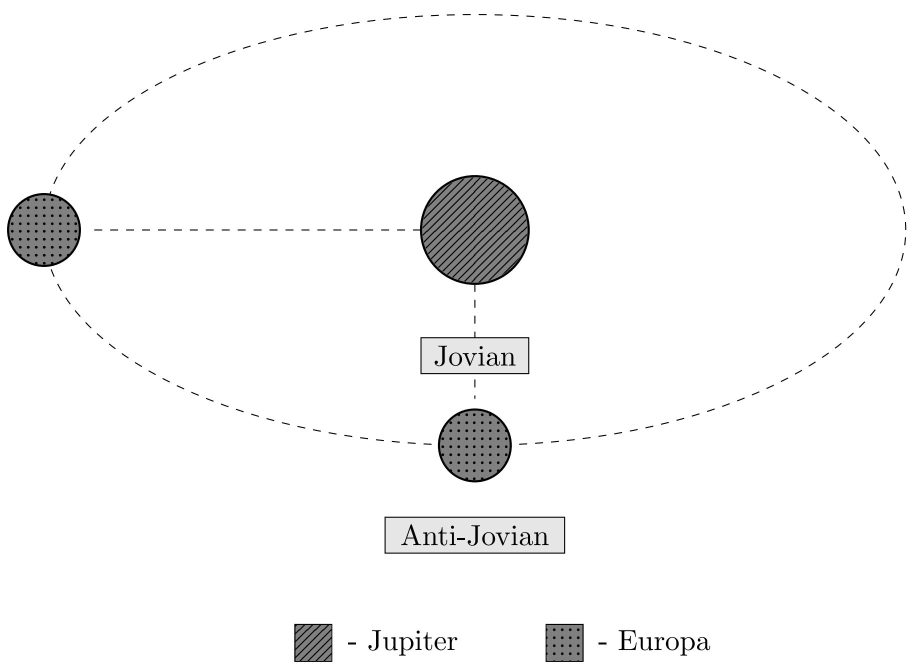

Fig 2: Elliptic orbit of Europa around Jupiter.

The eccentricity of Europa's orbit would normally decay away until it was circular if not for the effects of gravitational resonance [9]. In addition to the gravitational pull of Jupiter, Europa experiences significant forces from Ganymede, and Io, which are also Galilean moons. For every complete orbit of Ganymede, Europa completes two orbits while Io completes four orbits. This perpetual eccentricity and consequently, tidal heating, keeps Europa's ocean liquid and manifests even more distinctly on Io which is the most volcanically activate celestial body in our solar system.

If we look down at an equatorial cross section of Europa through a line that's perpendicular to the orbital plane of the moon, tidal heating would lead to colder temperatures at the Jovian and anti-Jovian points.

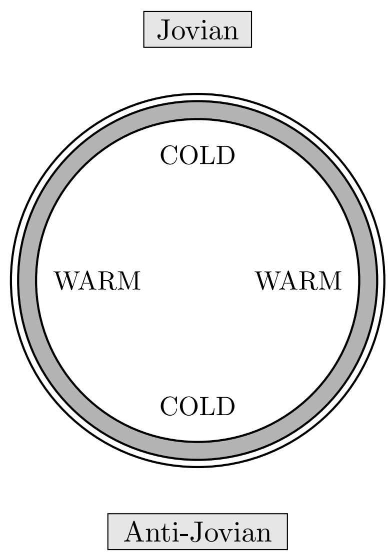

Fig 3: Expected temperature variation at the ocean floor due to tidal heating in the mantle.

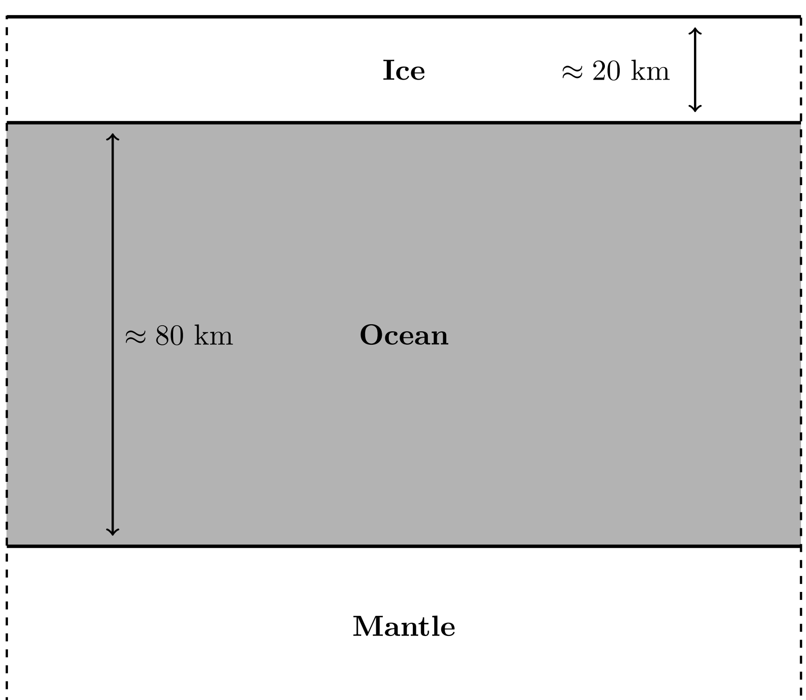

Fig 4: Rough structure of the ice-ocean system.

1.2 Research Aim

The aim of this project is to investigate the coupled ice-ocean dynamics influenced by an inhomogeneous temperature distribution that could be present on the ocean floor of an icy moon, due to tidal heating effects. We first benchmarked our code by comparing data in case where there is a homogeneous temperature distribution from *J. Purseed's* PhD thesis [10]. We then systematically varied the parameters of the system, including the ocean floor temperature distribution, to investigate their effects on the final state of the system.

1.3 Method

The ring-like ice-ocean system of Europa (of a 2D cross section, see **Fig 3**) was unwrapped and modelled as a periodic, rectangular domain.

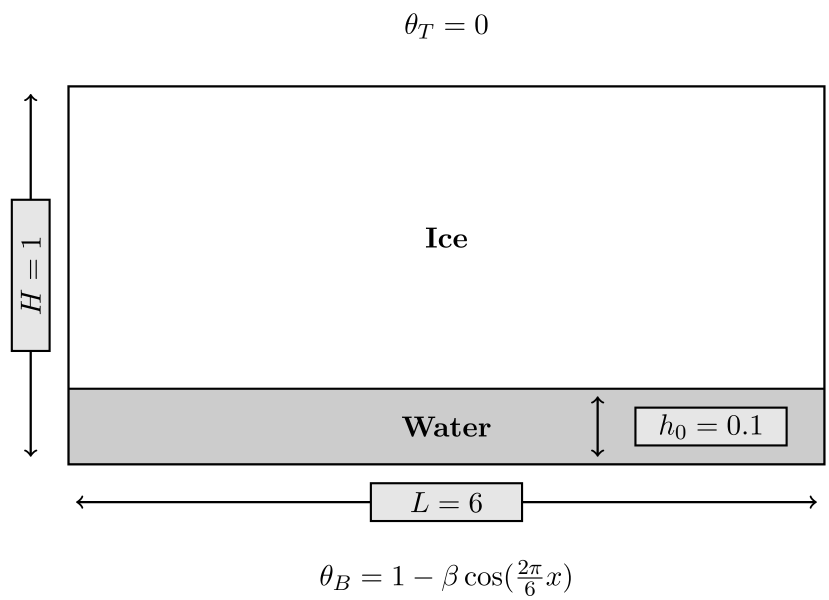

Fig 5: Diagram detailing the structure of the domain. H and L are the height and length of the domain, respectively. h_0 is the initial height of the ice-water interface. At all times we impose a temperature profile of θ_T and θ_B along the top and bottom boundaries, respectively. The horizontal axis is periodic to model the circular nature of the domain.

All the parameters have been non dimesionalised as given in *Purseed's* thesis (see their *chapter 2*) for convienience of comparison. Some important initial parameters that control the system are:

- θ_M - The melting temperature of the ice.
- β - The amplitude of the temperature variation at the ocean floor.
- Ra - The Rayleigh number of the system, which is the ratio of buoyancy forces to viscous forces.
- St - The Stefan number, which is the ratio of the thermal diffusivity to the latent heat of fusion.
- A - This is a parameter that controls the change in melting point due to pressure.

The existence of water and ice in the same system brings about another dimension of complication. This was handled by employing the phase field method as described in *E. Hester, et al, 2020* [4], which allows us to track the position of the ice-water interface. The code for the model was adapted from an implentation of this method in Dedalus v3[1], given to us by *Eric Hester*. A suite of analysis tools were created to accurately track the evolution of the system.

1.4 Fluid Instabilities

When a fluid system is heated from below, cooled from above, or both, a gravitationally unstable situation arises. Hot, less dense fluid tend to rise while cold, denser fluid sinks. If we impose a warm uniform temperature along the bottom boundary, and provided that the Rayleigh number of the system is sufficient, the system will form convection cells (see **Fig 6**). This is known as Rayleigh-Bénard convection. In our case, the convection cycles result in the formation of cavern structures in the ice, which in turn influence and lock the convection cells.

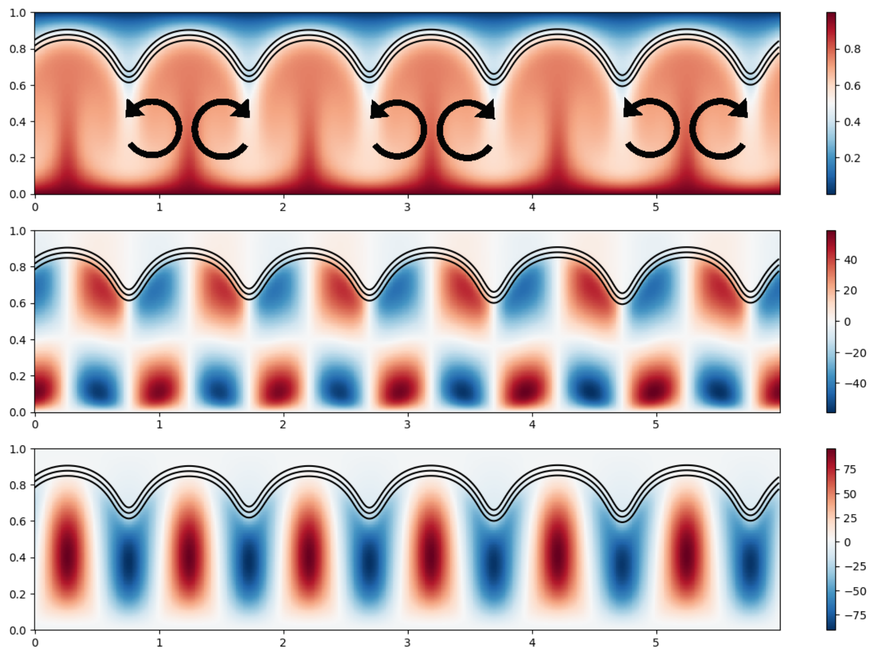

Fig 6: Simulation output showing mature Rayleigh–Bénard convection cycles inside ice caverns. From top to bottom the colours in the images represent: temperature, horizontal velocity, and vertical velocity. In each image the three lines represent the ice-ocean interface, with the ice layer above and the ocean below. The arrows show examples of fluid flow.

3 Horizontal Convection

Horizontal convection is a fluid instability formed due to regions of varying heat flux along a horizontal boundary [7]. It is present in many natural systems such as large scale oceanic currents, and the ocean currents underneath a glacier. If there is enough average heating for Rayleigh-Bénard convection to occur, **and** there are horizontal variations in this heating, then we can expect for the two types of convection to compete. The paper by *Couston, et al* [3] performed simulations with non-periodic boundaries and showed the competition of regimes, when subjected to a varying linear heat flux at the upper boundary, and a constant heat flux along the lower boundary.

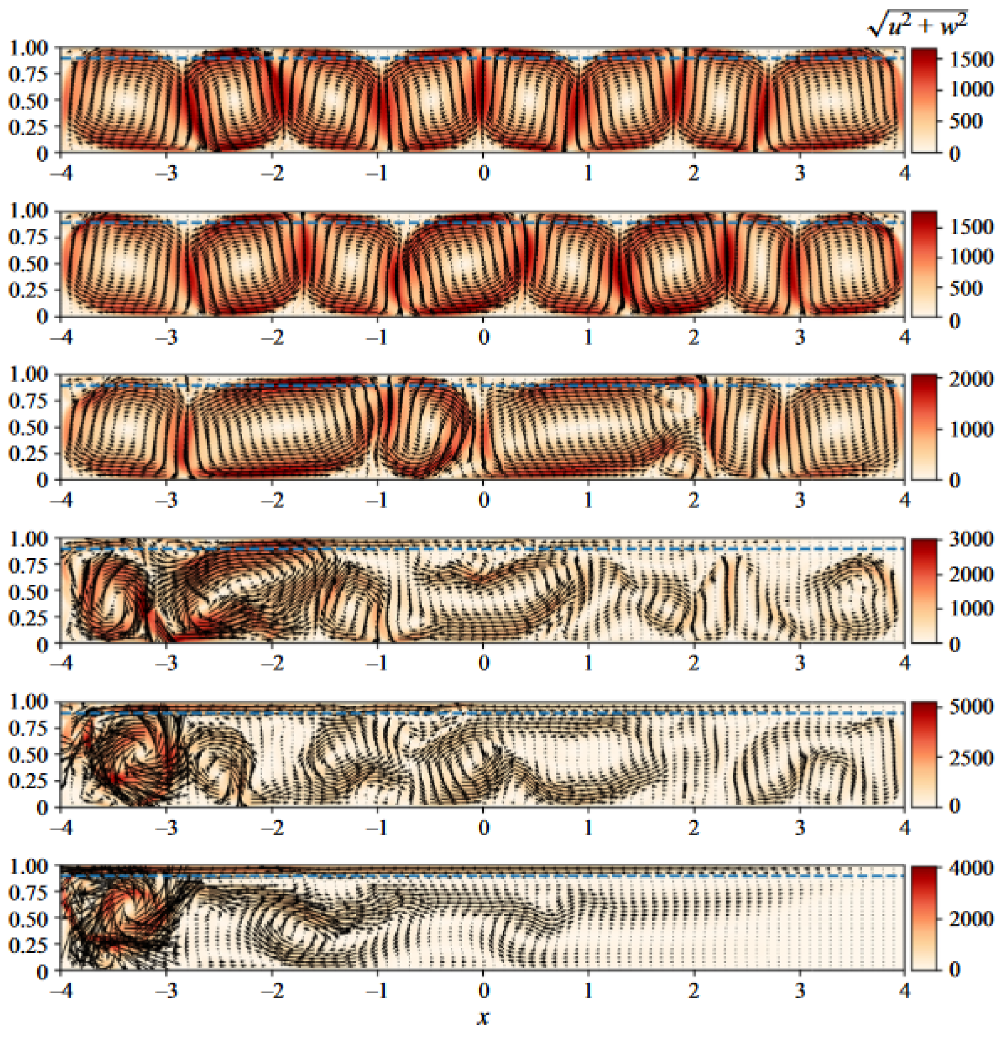

Fig 7: Image from *Couston's* paper (their *Figure 2*) showing, from top downwards, the regime change from Rayleigh-Bénard convection to horizontal convection when increasing the ratio of upper boundary heat flux variation to lower boundary constant heat flux. We can clearly see the decrease in number of individual convection cells and the formation of one giant convection cell.

As previously mentioned, the temperature at the ocean floor is given by $\theta_B(x) = 1 - \beta\cos(\frac{2\pi}{6}x)$. All experiments in this section used a Rayleigh number of $Ra = 10^5$.

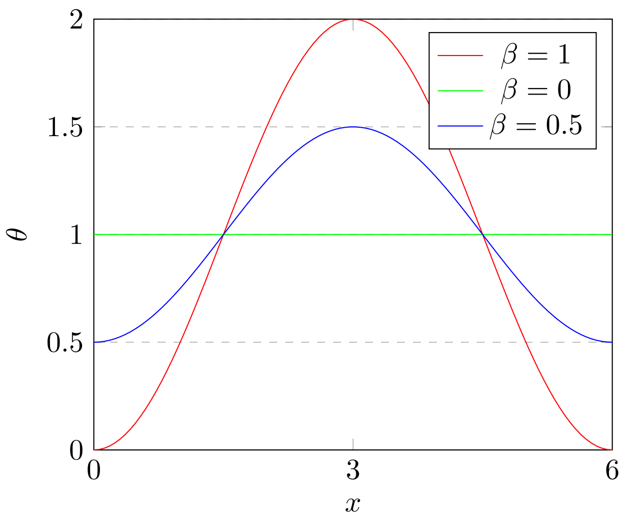

Fig 8: Temperature profile shape at the ocean floor. The temperature is warmest at the centre of the domain and coldest at the edges.

It is likely that having periodic boundaries in our model will change the dynamics of the system from *Couston's* simulations. We might expect that having solid walls in the non-periodic case would help produce a vertical current due to reaction forces. That being said, we did not investigate the difference between periodic and non-periodic boundaries in this project. Rather, we wanted to see how the ocean dynamics will change with a varying bottom temperature, and to investigate the sensitivity to the model's parameters. In addition to this, we did not apply a heat flux along our boundaries but rather a temperature profile.

3.1 Regime Classification

Since the system contains competing forms of convection, there is some ambiguity in defining what regime exists at equilibrium. In our project, we define a horizontal convection regime to consist of one cavern with two convection cycles inside it, like in **Fig 10**. Any deviation from this is defined as a Rayleigh–Bénard like regime. We say that a system reaches equilibrium when the average height of the ice-interface no longer changes, which all runs on this report achieve before the end of their runtime.

3.2 CASE I: Varying β

We first varied the bottom temperature amplitude to see how the system would react, and if it would transition from a Rayleigh–Bénard regime to a horizontal convection regime.

Table 1: Example parameters for CASE I. For the final state of 1A see **Fig 6**.

ID	**Runtime**	St	θ_M	h_0	β	A
1A (Control)	5	1	0.5	0.1	0	0
1B	5	1	0.5	0.1	0.2	0
1C	3	1	0.5	0.1	0.32	0
1D	3	1	0.5	0.1	0.36	0
1E	3	1	0.5	0.1	0.4	0
1F	3	1	0.5	0.1	0.6	0

For low values of β (**Figure 9**), the regime looks more like Rayleigh–Bénard convection (**Figure 6**) but with less cavern formation. Interestingly, after a certain point in some runs, we see caverns form at the horizontal edges. We then have a cavernous regions above a relatively cold region. Note that with our model, *higher β values will lead to a warmer central temperature but will also produce colder regions at the edges*, which may contribute to the lack of edge caverns at high β values.

When we reach larger values of β, the system forms something that may be more akin to horizontal convection (**Figure 10**). We found that the system forms one large cavern near the centre with two convection cycles within it. There's very little ice melting at the horizontal edges of the domain which makes sense as the temperature of the bottom boundary is lower in these regions. Further experimentation (1C-1D were done after the others) showed that the regime switches between $0.32 < \beta < 0.36$. We define low β as $\beta < 0.32$.

For higher values of β we see that the maximum height of the ice-water interface is always very close to the upper limit of the domain (**Figure 10**).

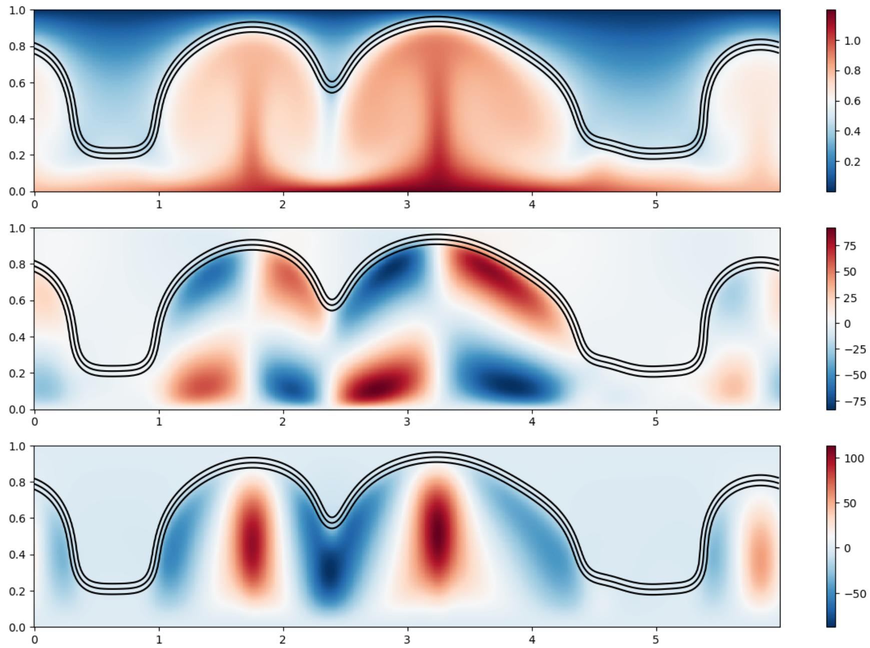

Fig 9: Final state of 1B and 2A ($\beta = 0.2$). The system initially had no caverns at the two horizontal edges of the domain but the structure kept expanding horizontally. From top to bottom, all figures in this format show: temperature distribution, horizontal velocity, vertical velocity.

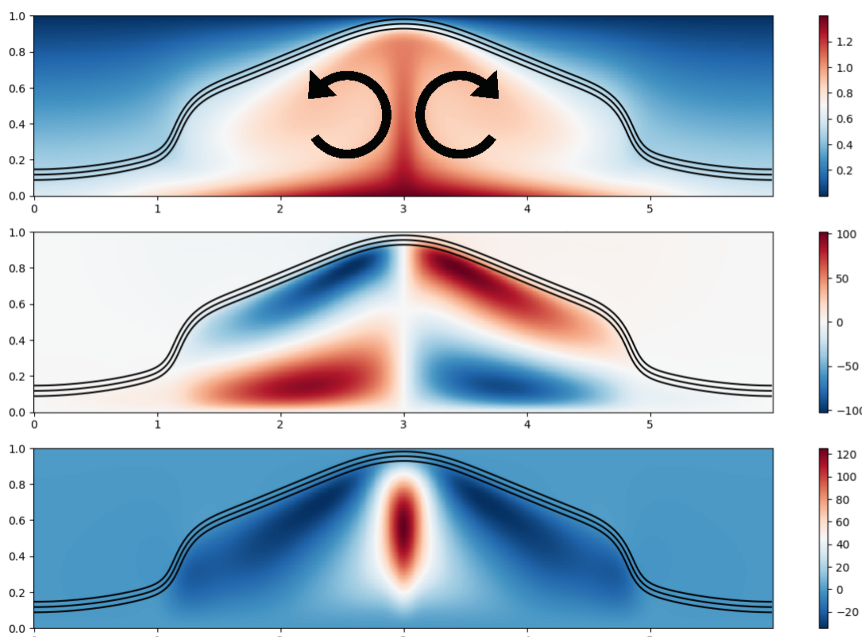

Fig 10: Final state of 1D and 3E ($\beta = 0.36$). We now see a single cavern forming near the centre with counter rotating convection cells inside it. This is a clear example of what we define to be a horizontal convection regime. The arrows show examples of fluid flow.

3.3 CASE II: Varying other parameters with low β

To test if the transition to horizontal convection only occurs beyond $\beta \geq 0.36$, we ran a few dozen experiments keeping $\beta = 0.2$ and varying other parameters. The point was to see if we could form a horizontal convection regime with low β values by changing the other parameters.

Table 2: Example parameters for CASE II. See **Fig 9** for the final state of 2A.

ID	**Runtime**	St	θ_M	h_0	β	A	**Purpose**
2A (Control)	5	1	0.5	0.1	0.2	0	Control
2B	3	1	0.5	0.1	0.2	0.5	Effect of A
2C	3	1	0.1	0.1	0.2	0	Effect of θ_M
2D	3	1	0.7	0.1	0.2	0	Effect of θ_M
2E	3	1	0.5	0.5	0.2	0	Effect of h_0
2F	5	20	0.5	0.1	0.2	0	Effect of St

We found that it was impossible to form a horizontal convection regime like the one in **Fig 10**, no matter what parameter was changed.

- **Changing A:** Increasing A seemed to decrease the asymptotic height of the system.
- **Changing θ_M:** Lowering θ_M increased the rate of ice melting and made the asymptotic height larger. Higher θ_M values had the opposite effect, and decreased the number of caverns.
- **Changing h_0:** This did not have a significant effect on the system. The final state of various runs with different h_0 values looked very similar, although with different numbers of caverns. There did not seem to be a correlation with cavern number and h_0.
- **Changing St:** This had a similar effect to changing the θ_M value. Higher St values decreased the number of caverns and the asymptotic height.

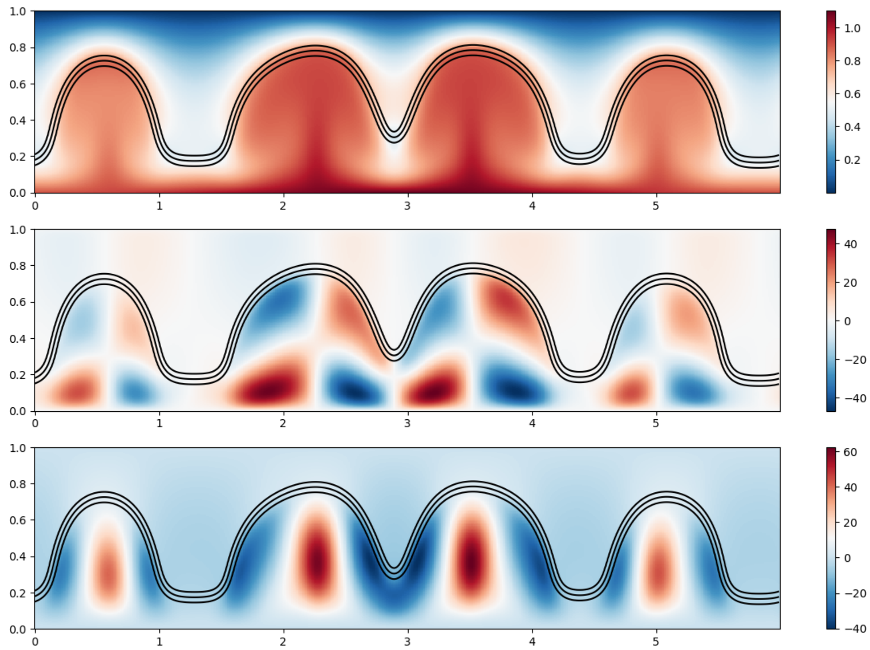

Fig 11: Final state of 2B which has a higher melting-point-pressure parameter ($A = 0.5$). We see that the asymptotic height is lower but the ice caverns roughly hold the same shape.

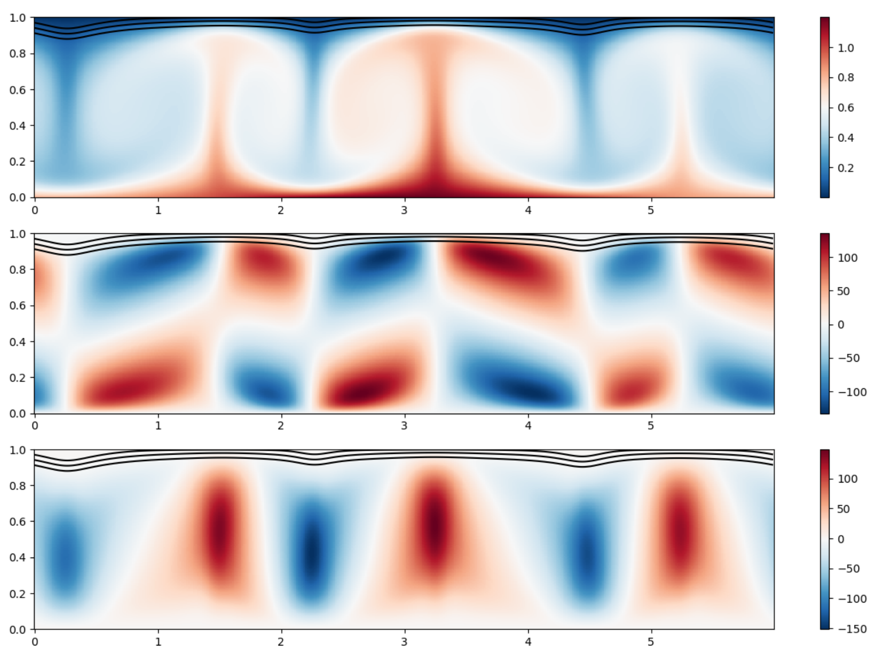

Fig 12: Final state of 2C which has a lower melting temperature ($\theta_M = 0.1$). The ice layer mostly melts away but the ice caverns roughly hold the same shape.

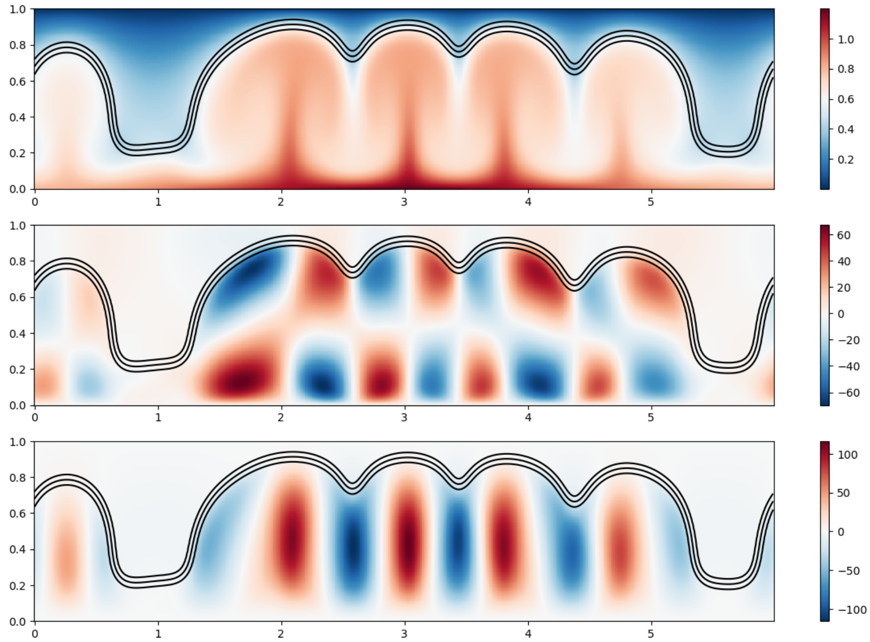

Fig 13: Final state of 2E which has a higher initial interface height ($h_0 = 0.5$). Much like 2A but with more caverns near the centre.

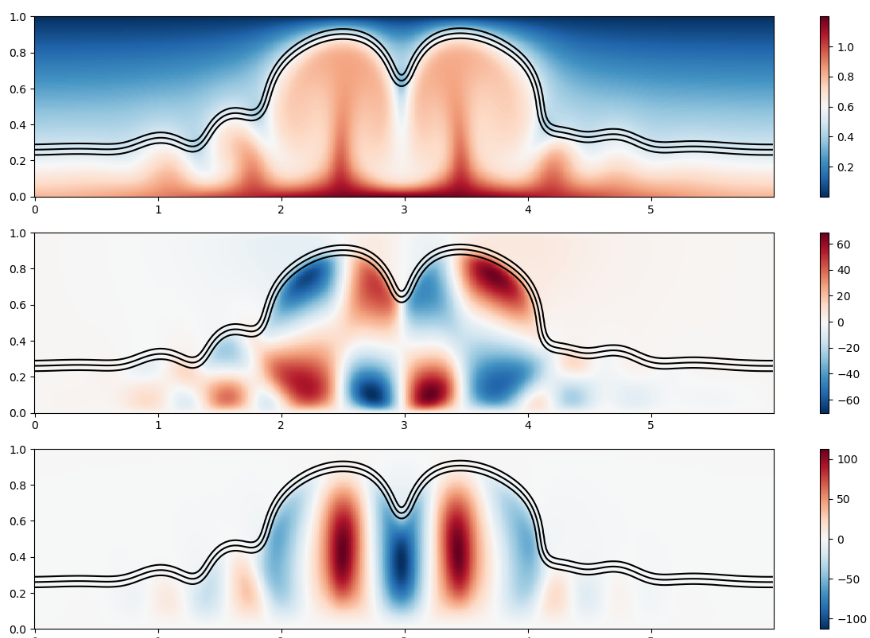

Fig 14: Final state of 2F which has a higher Stefan number ($St = 20$). We no longer see caverns at the edges and the ones that do form are localized to the centre.

3.4 CASE III: Varying θ_M with $\beta = 0.36$

We now wanted to see whether the horizontal convection regime would remain stable if we changed the melting point of the ice while keeping $\beta = 0.36$.

Table 3: Example parameters for CASE III.

ID	**Runtime**	St	θ_M	h_0	β	A
3A	3	1	0.1	0.1	0.36	0
3B	5	1	0.3	0.1	0.36	0
3C	3	1	0.35	0.1	0.36	0
3D	3	1	0.45	0.1	0.36	0
3E (Control)	3	1	0.5	0.1	0.36	0
3F	3	1	0.6	0.1	0.36	0

For low values of θ_M, the final states are horizontal convection regimes (**Figure 15**). So is the case for very large values of θ_M (**Figure 17**). Unexpectedly, the system seems to switch to a Rayleigh–Bénard like regime between $0.3 \geq \theta_M \geq 0.5$ (**Figure 16**).

We repeated the experiments once more to make sure that this isn't an erroneous result and found that the system does indeed switch between the two regimes. In fact, when the experiment was repeated with $\beta = 0.4$, the same transient behaviour was observed. However the window in which the transient behaviour occurs is much smaller.

When we attempted to recreate the results with $\beta = 0.6$ we found that the system always ended up with a horizontal convection regime. Although it is possible that our resolution of θ_M values was too coarse to capture the transient window.

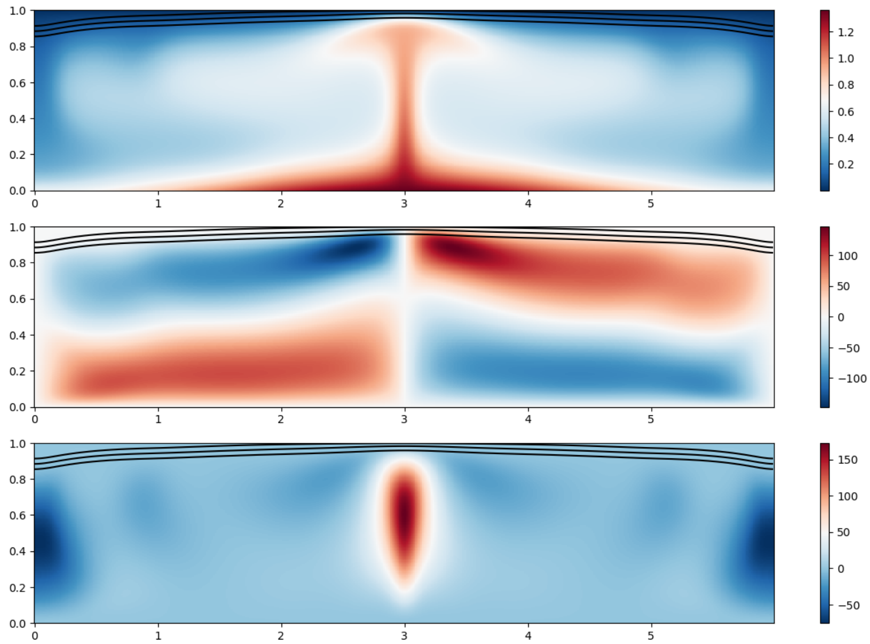

Fig 15: Final state of 3A which has a low θ_M ($\theta_M = 0.1$). We see a horizontal convection regime.

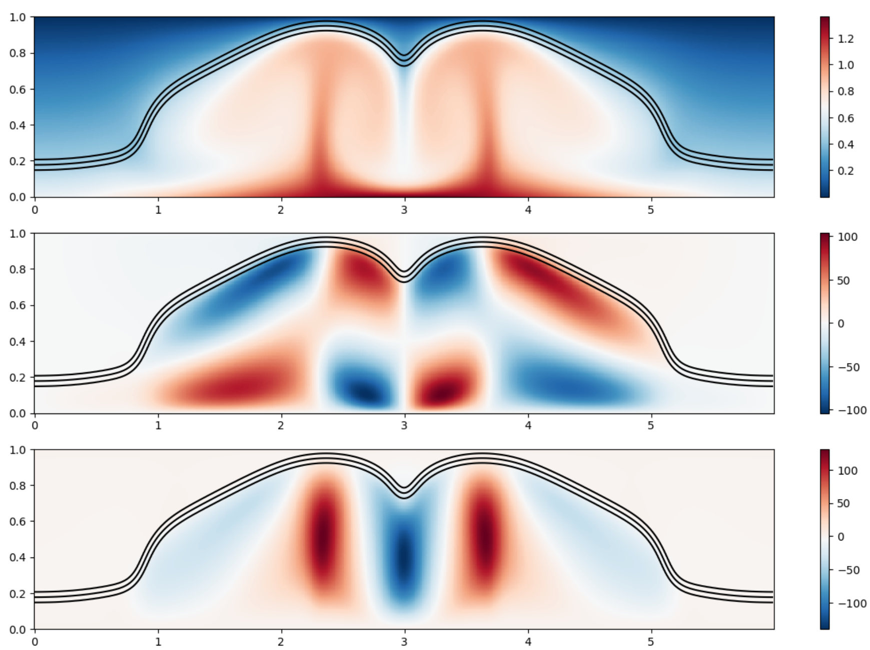

Fig 16: Final state of 3D which has $\theta_M = 0.45$. We see a Rayleigh–Bénard like regime.

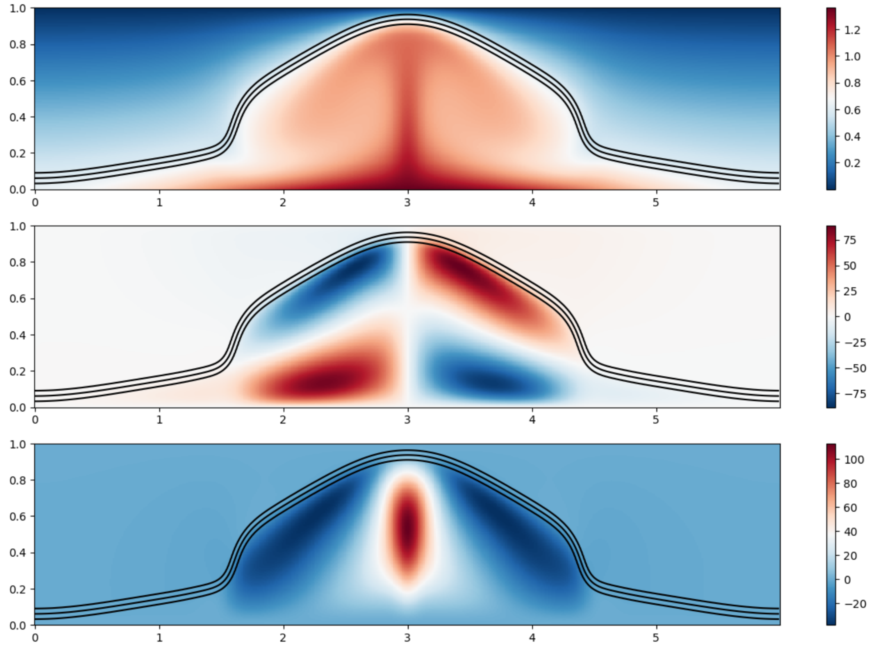

Fig 17: Final state of 3F which has a high θ_M ($\theta_M = 0.6$). We see a horizontal convection regime again.

In **Fig 16** we see that there is a strong downward current at the centre of the domain, even though we expect a rising current due to the warmer bottom temperature imposed at the centre and the fact hot fluids are less dense. As mentioned before, the ice caverns have a locking effect on convection cells. At higher θ_M values, we find that the central ice-dip that we see in **Fig 16** at $x = 3$ doesn't ever form. At lower θ_M values, the ice-dip does form but melts away quickly letting the convection cells to merge.

It's possible that at $\beta = 0.36$, the system still prefers to be in a Rayleigh–Bénard like regime but I hypothesized that if we were to initialize the simulation with a single cavern, the system would end up with a horizontal convection regime. It was also possible that Rayleigh –Bénard convection would be induced at $\beta = 0.6$ if we initialized the simulation with a dip at the centre. To test this hypothesis, two experiments were performed: trying to induce horizontal convection at $\theta_M = 0.35$ where we would expect the system to be in a Rayleigh–Bénard like regime, and trying to induce Rayleigh–Bénard convection at $\theta_M = 0.6$ where we would expect the system to be in a horizontal convection regime.

To induce horizontal convection in a system where would expect a Rayleigh–Bénard regime, we changed the initial ice topology to have a cavern structure at the centre (**Figure 18**). This was accomplished by adding a Gaussian mask.

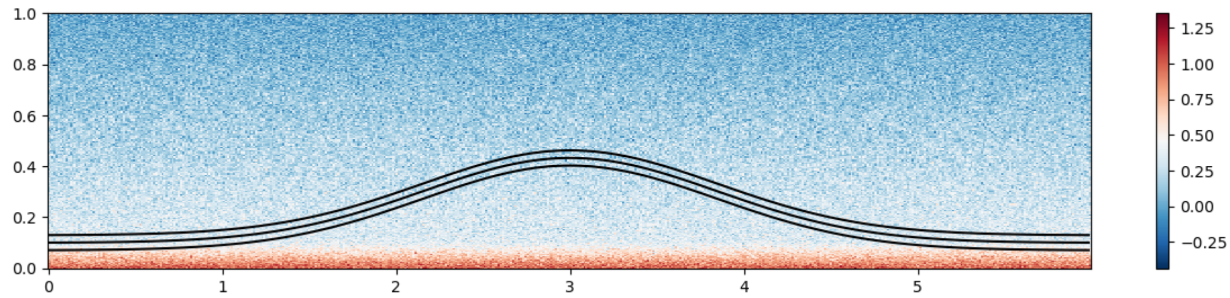

Fig 18: The initial cavern structure used.

All the other parameters are as 3C in **Table 6**. The final state of this system is indeed a horizontal convection regime as shown in **Figure 19**. This demonstrates that the initial ice topology has a strong effect on the ocean circulation and the final equilibrium state reached.

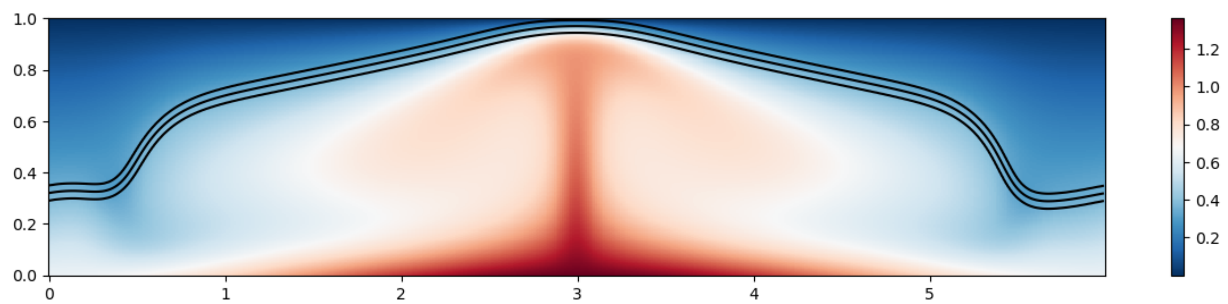

Fig 19: Final temperature distribution state of a simulation initialized with a single cavern as shown in **Fig 18**. The parameters are otherwise the same as for **Fig 16**

We then tried to induce a Rayleigh–Bénard regime at $\beta = 0.6$ by changing the initial ice topology to have a dip at the centre, surrounded by two caverns. This was accomplished by adding three Gaussian profiles, two at $x = 2.5$ and $x = 3.5$ for the caverns, and one at $x = 3$ for the dip.

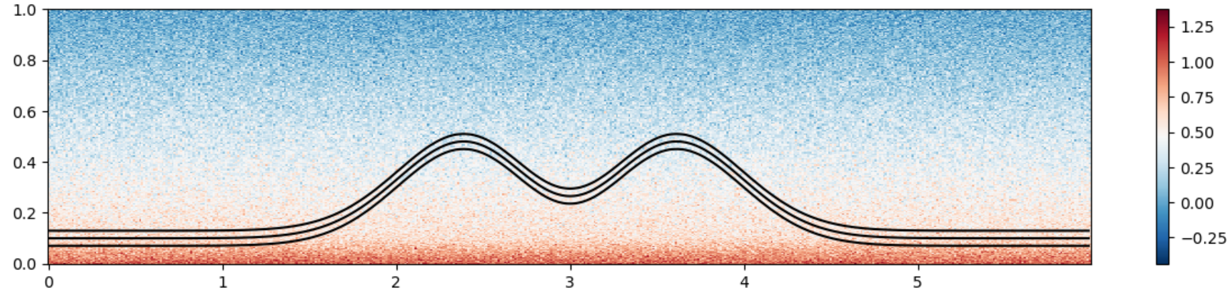

Fig 20: The initial ice topology used to test the second experiment.

We find that the system still ends up in a horizontal convection regime. It is possible, however unlikely, that a larger dip is needed to induce a Rayleigh-Bénard regime. This suggests an enhanced stability of the horizontal convection regime, compared with the Rayleigh–Bénard regime, which does not persist when perturbed.

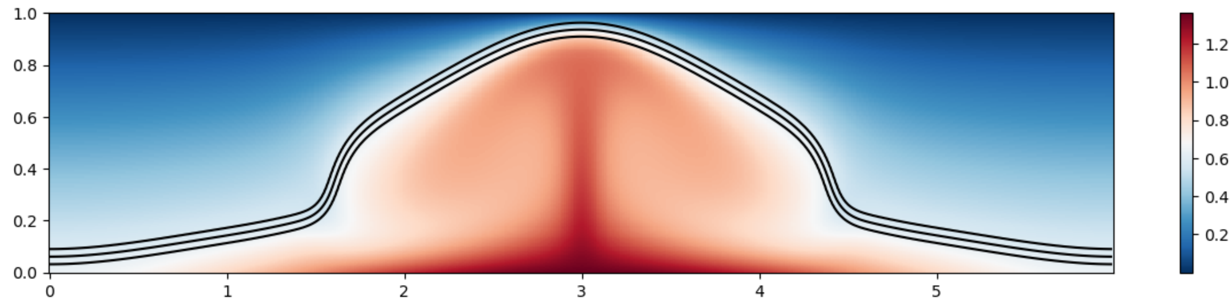

Fig 21: Final temperature distribution state of **Fig 20**.

5 Conclusions

CASE I varied the amplitude of the bottom temperature variation, while keeping the other parameters constant. Here we saw that the system switches regimes from Rayleigh-Bénard to horizontal convection between $0.32 < \beta \leq 0.34$. CASE II used a low β value and varied the other parameters to see if we could induce horizontal convection. We found that this could not be done. CASE III investigated if the horizontal convection regime at $\beta = 0.36$ was stable when changing the melting temperature. Here we found that at low and high θ_M values, the system ends up in horizontal convection regimes. For a set of mid θ_M values which we call the transient window, the system forms Rayleigh-Bénard convection regimes. We repeated the experiment with the same parameters, and also a higher β value, and found that the trend was present. At very high β values, we do not observe this switching of regimes and only find a horizontal convection system. A possible explanation for the transient window was given. We then did some tests which give and take credence from this explanation, although further investigation is necessary.

It is evident that the system is very sensitive to the parameters used and finding an overarching theory that can describe the evolution of the system is a difficult task. That being said we have shown some general trends of the system when all parameters but one are fixed, and some unusual behaviours such as Rayleigh-Bénard locking at relatively high β that can be investigated further.

References

[1] K J Burns, G M Vasil, J S Oishi, D Lecoanet, B P Brown, ”Dedalus: A Flexible Framework for Numerical Simulations with Spectral Methods,” Physical Review Research, vol. 2, no. 2, Apr. 2020.

[2] Chang, S. (2019). Rayleigh-Bénard Convection. [online] www.terpconnect.umd.edu. Available at: https://www.terpconnect.umd.edu/ dsvolpe/TREND/2019/Media/ Chang/convection.html.

[3] Louis-Alexandre Couston, Nandaha, J. and Favier, B. (2022). Competition between Rayleigh-Bénard and horizontal convection. Journal of Fluid Mechanics, 947.
doi:https://doi.org/10.1017/jfm.2022.613.

[4] Hester EW, Couston L-A, Favier B, Burns KJ, Vasil GM. 2020 Improved phase-field models of melting and dissolution in multi-component flows. Proc. R. Soc. A 476: 20200508. http://dx.doi.org/10.1098/rspa.2020.050

[5] Hurford, T.A.; Sarid, A.R.; Greenberg, R. (January 2007). ”Cycloidal cracks on Europa: Improved modeling and non-synchronous rotation implications”. Icarus. 186 (1): 218-233.

[6] Khurana, K., Kivelson, M., Stevenson, D. et al. Induced magnetic fields as evidence for subsurface oceans in Europa and Callisto. Nature 395, 777-780 (1998). https://doi.org/10.1038/27394

[7] Max Planck Institute, Dept. of Fluid Physics (2016). Horizontal convection. [online] Ds.mpg.de. Available at: https://www.lfpn.ds.mpg.de/shishkina/projects/ horizontal__convection.html.

[8] NASA (n.d.). Europa Tide Movie. [online] NASA’s Europa Clipper.
Available at: https://europa.nasa.gov/resources/52/europa-tide-movie/.

[9] NASA (n.d.). Europa: Facts - NASA Science. [online] science.nasa.gov.
Available at: https://science.nasa.gov/jupiter/moons/europa/europa-facts/.

[10] Purseed, J. (2020). Interaction between a melting boundary and a convective flow: a numerical study. PhD Thesis.

[11] Soderlund, et al (2020). Ice-Ocean Exchange Processes in the Jovian and Saturnian Satellites. Space Science Reviews, 216(5).
doi:https://doi.org/10.1007/s11214-020-00706-6.